Article

Discovery Medicine 2026; 38(211): 2469–2479
https://doi.org/10.24976/Discov.Med.202638211.195

Breviscapine Blunts Hypertrophic Scar Formation via Dual Suppression of TGF-β1 Signaling and the Akt-mTOR Pathway

Peng Guo[1], Qianqian Gao[2], Li Lin[2,*]

[1]Tuina Department, Shandong Provincial Hospital Affiliated to Shandong First Medical University, 250021 Jinan, Shandong, China
[2]Department of Plastic Surgery, Shandong Provincial Hospital Affiliated to Shandong First Medical University, 250021 Jinan, Shandong, China
*Correspondence: Lingling_Lw1@163.com (Li Lin)
Submitted: 16 January 2026 Revised: 24 April 2026 Accepted: 1 June 2026 Published: 24 August 2026

Background: Hypertrophic scar (HS) arises from aberrant cutaneous wound healing, characterized by uncontrolled myofibroblast proliferation and disproportionate extracellular matrix (ECM) accumulation. Breviscapine, a natural compound, suppresses inflammation and fibrosis. This study aimed to evaluate breviscapine as a therapeutic avenue against HS and unravel its molecular basis.

Methods: *In vivo*, a rabbit ear HS model was established and treated with different doses of breviscapine. Scar morphology was macroscopically evaluated. Fibrosis-related markers (collagen type I alpha 1 [COL1A1], collagen type III alpha 1 [COL3A1], actin alpha 1, skeletal muscle [ACTA1], alpha-smooth muscle actin [α-SMA]) were quantified by quantitative real-time PCR (qRT-PCR) and Western blotting. α-SMA expression, collagen fiber organization and transforming growth factor-β1 (TGF-β1) levels were assessed by immunofluorescence staining, Masson staining, and immunohistochemistry/Western blotting, respectively. *In vitro*, HS fibroblasts (HSFs) were exposed to breviscapine, and cell counting kit-8 (CCK-8) assay, Sirius red staining and Western blotting were separately performed to determine cell viability, collagen production, and the expression of fibrosis-related markers, TGF-β1, and the Akt-mTOR pathway.

Results: *In vivo*, breviscapine treatment attenuated rabbit ear scar formation, while diminishing COL1A1/COL3A1/ACTA1 mRNA levels and collagen I/collagen III/α-SMA/TGF-β1 protein levels and improving collagen fiber density and arrangement ($p < 0.001$). *In vitro*, breviscapine inhibited HSF viability, reversed TGF-β1-stimulated collagen overproduction, and suppressed the protein expression of fibrosis-related markers ($p < 0.05$). Notably, breviscapine attenuated the protein expression of TGF-β1 and the Akt-mTOR pathway in HSFs ($p < 0.01$).

Conclusion: Breviscapine exerts anti-HS effects by targeting the TGF-β1 signaling and the Akt-mTOR pathway, providing a novel natural therapeutic candidate for HS management with anti-fibrotic, anti-proliferative, and pathway-targeted effects. Further investigation is warranted to validate its efficacy in clinical settings and to explore its long-term safety and optimal delivery strategies.

Keywords: hypertrophic scar; breviscapine; transforming growth factor-β1; Akt-mTOR pathway; collagen fiber

Introduction

Hypertrophic scar (HS), an extremely common dermal fibroblast hyperplasia, occurs frequently after burns, surgery or other trauma that affects the deep dermis [1,2], and is mainly manifested by excessive collagen and massive deposition of extracellular matrix [3,4]. The advancement of medical technology has yielded different therapeutic avenues for HS, with artesunate, silicone gel sheeting, intralesional bleomycin and pulsed laser as the mainstream [5–7]. However, a long-term systematic study revealed that HS is characterized by an extremely high recurrence rate and a lack of curative treatment [8]. Consequently, developing novel, effective therapeutic strategies remains a clinical priority for enhancing the survival environment for HS patients [9].

Transforming growth factor-β1 (TGF-β1) is pivotal in wound healing and HS formation [10]. A previous study showed that TGF-β1 increased the production of fibronectin and collagen in cultured epithelial cells via transcriptionally activating corresponding genes. The subcutaneous injection of TGF-β could effectively promote not only collagen accumulation but also fibrotic tissue responses [11]. Notably, TGF-β1 expression is increased in pathological scar fibroblasts [12,13]. Recent research has highlighted TGF-β1 as a therapeutic target to decipher the roles of specific genes and agents, such as botulinum toxin type A, in HS formation [13,14]. Beyond TGF-β1, emerging evidence underscored the significance of the phosphatidylinositol 3-kinase (PI3K)/Akt and the mechanistic target of rapamycin (mTOR) signaling path-

Copyright: © 2026 The Author(s). Published by Discovery Medicine. This is an open access article under the CC BY 4.0 license.
Note: *Discovery Medicine* stays neutral with regard to jurisdictional claims in published maps and institutional affiliations.

ways in HS progression. The Akt-mTOR pathway is a key regulator of cell proliferation, survival, protein synthesis, and autophagy. Existing studies have shown that inhibiting the Akt/mTOR pathway activation blocks proliferation, migration, extracellular matrix deposition and fibrosis of HS fibroblasts [15–18]. TGF-β1 can activate the Akt-mTOR cascade, which in turn stabilizes the myofibroblast phenotype and fuels a pro-fibrotic feedback loop [19]. This crosstalk between TGF-β1 and Akt-mTOR signaling presents a promising multi-target intervention point for anti-fibrotic therapy.

As reported, the mainstream agents for HS are classified into two types, adrenocorticosteroids and anti-tumor drugs [20,21]. However, their clinical application is limited by side effects, underscoring the urgent need for safer and more effective therapeutic agents with improved safety profiles. Breviscapine is isolated from the distinctive flavonoid herb, breviscapus, which is known for anti-inflammatory and anti-fibrotic properties but low systemic toxicity [22–25]. In recent years, it has attracted much attention by virtue of its valuable functions, including but not limited to promoting microcirculation, lessening blood viscosity, enhancing fibrinolysis and inhibiting cancer [22]. Therefore, breviscapine has been widely used not only in treating cerebral infarction and hypertension, but also in suppressing the development of tumors through inhibition of proliferation and angiogenesis [26]. In addition, preliminary research suggested that breviscapine can modulate both the TGF-β1 and Akt pathways in some diseases [23]. However, its specific effects on HS and the underlying mechanisms, particularly those concerning the TGF-β1/Akt-mTOR signaling axis, remain entirely unexplored. To our knowledge, this study is the first to investigate the therapeutic potential of breviscapine in HS and to verify the novel hypothesis that its efficacy is related to the concurrent inhibition of TGF-β1 and Akt-mTOR signaling pathways. By elucidating this dual-pathway mechanism, our research aims to position breviscapine as a novel, multi-target natural candidate for HS management.

Materials and Methods

Ethics Statement

As per current regulations and standards of the China Council on Animal Care and Use, all experimental animals were raised in solitary cages. Male New Zealand white rabbits (aged 3 months, n = 30, 2.5–3.0 kg, Shanghai SLAC Laboratory Animal Co., Ltd., China) were maintained at 25 °C and 55% humidity with a 12-h light/dark cycle and *ad libitum* access to food and water. The experimental protocol was approved by the Laboratory Animal Ethics Review Committee of Shandong Provincial Hospital Affiliated to Shandong First Medical University (No. HSRF (preliminary application) 2024-0027). All possible steps were taken to actively minimize animal suffering and discomfort.

Rabbit Ear HS Model Establishment and Therapy

The rabbit ear HS model was employed owing to its well-established relevance for investigating human HS pathophysiology [27]. This model reliably reproduces key features of human HS, including prolonged inflammation, excessive collagen deposition, and raised scar morphology. Based on the established methodology, the rabbit ear HS model was established. Briefly, 30 rabbits were allocated into five groups (n = 6 per group) using a random number table: control, HS, breviscapine-low dose (BE-L), breviscapine-medium dose (BE-M) and breviscapine-high dose (BE-H). Breviscapine (WKQ-0004798-20 mg, Chengdu Biaoxiang Biological Technology Co., Ltd., China) was dissolved in DMSO (D8370, Solarbio, China).

For modeling, rabbits were anesthetized with 1% pentobarbital sodium (30 mg/kg; STY667, Zzsiji, China). On the ventral side of every single ear, the epidermis, dermis and perichondrium were carefully removed. Then six circular full-thickness wounds (diameter: 10 mm) were created to build an HS rabbit ear model. On postoperative day 14, the wounds were completely re-epithelialized. Based on a previous study [28], breviscapine was administered at three doses: 5, 10, and 20 mg/kg. In the BE-L, BE-M and BE-H groups, after modeling, 5, 10, and 20 mg/kg breviscapine (0.2 mL) were subcutaneously injected into the rabbit ear on the 14th day (once a week; 4 times), respectively. The control rabbits received no treatment. Post-experimentally, the rabbits were euthanized by intravenous injection of an excessive dose of 1% pentobarbital sodium (STY667, Zzsiji, China) (150 mg/kg), in line with the 3R principle of animal experiments. Next, HS tissues were harvested for subsequent tissue and molecular analyses.

Cell Culture

Human HS fibroblasts (HSFs, XG-X4642, Shanghai Sig Biotechnology Co., Ltd., China) were confirmed to be mycoplasma-free and authenticated by STR detection. HSFs were cultured (37 °C) in a humidified 5% CO_2 incubator (E2398, Beyotime, China) with Dulbecco's Modified Eagle's Medium (DMEM, 30-2020, ATCC, USA) containing 10% fetal bovine serum (FBS, 30-2020, ATCC, USA).

Cell Viability Assay

Following cell exposure to breviscapine at 0, 2.5, 5, 10 or 15 µM, cell viability was determined using Cell Counting Kit-8 (CCK-8, ab228554, Abcam, UK). Briefly, cells in a 96-well plate were treated with 100 µL CCK-8 solution (37 °C, 5% CO_2, 3 h, in the dark), and observed at time points of 24 and 48 h. Afterwards, relative cell viability was examined using a microplate reader (SpectraMax 190, Molecular Devices, USA) at 460 nm.

Cell Grouping

Combining existing methodology and the results of cell treatment [13], a 48-h exposure to 15 µM breviscapine was therefore selected for subsequent experiments. After much deliberation, HSFs were assigned into control (normal culture), TGF-β1 (48-h stimulation of TGF-β1 (0.08 nM; HY-P7118, MCE, USA)), and TGF-β1+BE (48-h co-stimulation of 15 µM breviscapine and TGF-β1) groups.

Quantitative Real-Time PCR (qRT-PCR)

Total RNA was extracted from tissues by TRIzol Reagent (15596018, Romics, China), and transcribed into cDNA by PrimeScript RT reagent Kit (Perfect Real Time) (RR037B, Takara Biotechnology, Japan). SYBR Green Real-time PCR Master Mix (XY-9A-QPK-201, XYBiotechnology, China) was utilized with the ABI 7500 thermocycler (Shanghai Tusen Vision Technology, China) for quantifying collagen type I alpha 1 (COL1A1), collagen type III alpha 1 (COL3A1) and actin alpha 1, skeletal muscle (ACTA1). The primers are listed 5′ to 3′ as follows: COL1A1 (F) CATAAAGGGTCACCGTGGCT, (R) GTCATCTGCCCGGTAGTAGC; COL3A1 (F) AACAATGGTAGTCCTGGCGG, (R) CACCGTTCTTACCGGGTTCA; ACTA1 (F) GAGCGCAGCAGAAACCAGA, (R) TTACCAGGCCAGAGCCATTG; β-actin (F) ATTCATGCGGCCAAAGAGGA, (R) GAGCGCCAAATCAAGCAGAG. β-actin was used to normalize the relative expression of the three genes. The experiment was repeated in triplicate, and the relative fold-change was calculated using the $2^{-\Delta\Delta Ct}$ method [29].

Western Blotting

Cellular proteins and proteins in tissues (WB Super RIPA Lysis Buffer; XY9501, XYBiotechnology, China) underwent concentration measurement, where Collagen I, Collagen III, alpha-smooth muscle actin (α-SMA), TGF-β1, phosphorylated-Akt (p-Akt), Akt, mammalian target of rapamycin (mTOR), phosphorylated mammalian target of rapamycin (p-mTOR) and β-actin were measured with BCA Assay Kit (P0012, Beyotime, China). Equal amounts of protein samples were separated by electrophoresis on 6% sodium dodecyl sulfate-polyacrylamide (SDS-PAGE) gels (P0676-500 mL, Beyotime, China), and subsequently transferred onto PVDF membranes (10600023, Cytiva, China). Primary antibody information is as follows: TGF-β1 (MA5-16949, 1:1000, 50 kDa, Invitrogen, USA), collagen I (14695-1-AP, 1:3000, 130 kDa, Proteintech, USA), collagen III (68320-1-Ig, 1:5000, 139 kDa, Proteintech, USA), α-SMA (67735-1-Ig, 1:6000, 43 kDa, Proteintech, USA), p-Akt (#4060, 1:2000, 60 kDa, CST, USA), Akt (#4685, 1:1000, 60 kDa, CST, USA), mTOR (#2983, 1:1000, 289 kDa, CST, USA), p-mTOR (#5536, 1:1000, 289 kDa, CST, USA), β-actin (MA5-15739-HRP, 1:900, 42 kDa, Invitrogen, USA). Secondary antibody information is as follows: Goat Anti-Mouse IgG H&L (ab205719, 1:7000, Abcam, UK), Goat Anti-Rabbit IgG H&L (ab205718, 1:3000, Abcam, UK). All these primary antibodies were incubated with membranes (4 °C, overnight). After washing with TBST (B1009-TBST, APPLYGEN, China) thrice, the membranes were separately incubated with their corresponding secondary antibody at room temperature (RT) for 1 h. Protein bands were visualized using an Efficient Chemiluminescence (ECL) Kit (10145-100 mL, Proand, China) and scanned using an ImageQuant densitometric scanner (BH-2, OLYMPUS, Japan), followed by quantification using ImageJ (version 1.52; National Institutes of Health, Bethesda, MD, USA) software. Every experiment was conducted three times.

Immunofluorescence Staining Assay

α-SMA expression was measured using immunofluorescence staining *in vivo*, after 28-day treatment with breviscapine. First, tissues were fixed with 4% paraformaldehyde (G0528, GBCBIO, China) (10 min), rinsed with PBS (C0221A, Beyotime, Shanghai, China), permeabilized using 0.1% Triton X-100 (C03-03003, Bioss, USA) (15 min), and blocked in 5% bovine serum albumin (BSA, A4628-100ML, Sigma-Aldrich, USA) (1 h). Next, the tissues were incubated with diluted alpha smooth muscle actin Polyclonal antibody (14395-1-AP, 1:350, 43 kDa, Proteintech, USA) (overnight, RT), washed 3 times with PBS, and then incubated with Goat Anti-Rabbit IgG H&L (ab205718, 1:3000, Abcam, UK) (RT, 1 h). DAPI (4083S, CST, USA) was used for nuclear staining. Using a microscope (E400, Nikon, Japan), the images of the wound area (magnification ×400, scale bar = 50 µm) were immediately dissected using Image-Pro Plus 6.0 software (Media Cybernetics, Rockville, MD, USA).

Masson Staining Assay

Trichrome Stains (Masson) (HT15), comprising Biebrich Scarlet-Acid Fuchsin Solution, Working Phosphotungstic, Phosphomolybdic Acid Solution and Aniline Blue Solution, was used to detect collagen fibers. Initially, the slices were deparaffinized, rehydrated with distilled water, incubated with preheated Bouin's solution (HT10132) (56 °C, 15 min), and then cooled in tap water (20 °C). After thorough washing to remove yellow coloration, the slices were stained with Weigert's iron hematoxylin solution (HT1079) (5 min), and rinsed in tap water (5 min) followed by deionized water (SL2240-100 mL, Coolaber, China). Later, color development with Biebrich Scarlet-Acid Fuchsin Solution (5 min) and washing with deionized water were performed. Subsequently, the slices were immersed in Working Phosphotungstic/Phosphomolybdic Acid Solution (5 min), dyed with Aniline Blue Solution (5 min), and immersed in Acetic Acid (45745) diluted to 1% (2 min). After dehydration in an alcohol series, the slides were dehydrated and mounted. All the reagents except deionized water were obtained from Sigma-Aldrich (USA). Besides,

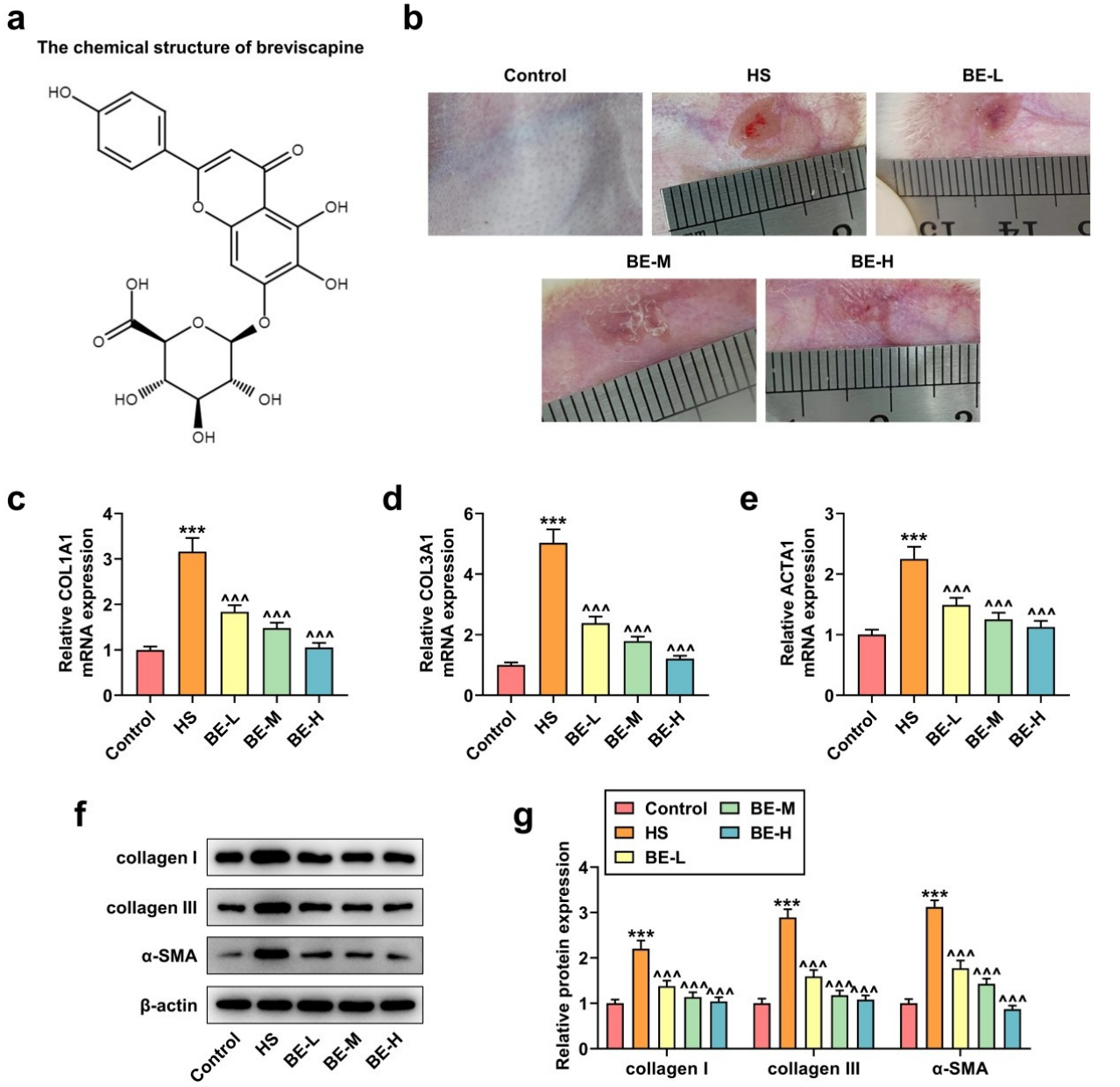

Fig. 1. The effects of breviscapine on scar appearance and the mRNA and protein expression of fibrosis-related markers *in vivo*. (a) The chemical structure of breviscapine. (b) The appearance of scar tissues after 28-day treatment with breviscapine on the rabbit ear HS model, including the control (n = 6), HS (n = 6), BE-L (n = 6), BE-M (n = 6), and BE-H groups (n = 6). (c–e) The mRNA expression levels of fibrosis-related markers (collagen type I alpha 1 (COL1A1), collagen type I alpha 1 (COL3A1), actin alpha 1, skeletal muscle (ACTA1) (qRT-PCR, β-actin as the internal reference). (f,g) The protein expression levels of fibrosis-related markers (collagen I, collagen III, and alpha-smooth muscle actin (α-SMA)) (Western blotting, β-actin as the housekeeping gene). All experiments were performed in triplicate, with data presented as mean $\pm$ SD (n = 6 rabbits/group). $^{***}p < 0.001$ vs. Control; $^{\wedge\wedge\wedge}p < 0.001$ vs. HS. Abbreviation: HS, hypertrophic scar; BE-L, breviscapine-low dose; BE-M, breviscapine-medium dose; BE-H, breviscapine-high dose; qRT-PCR, quantitative real-time PCR.

the images depicting the wound area (magnification $\times$100, scale bar = 50 µm) were observed under the microscope using the Image-Pro Plus 6.0 software (Media Cybernetics, Rockville, MD, USA).

Immunohistochemical Assay

Prior to immunohistochemistry, 5 µm scar tissue sections were prepared. After deparaffinization and dehydration, antigenic repair was performed. Next, the sections were exposed to 3% hydrogen peroxide (10 min), blocked with BSA (RT, 10 min), and incubated with

diluted TGF beta-1 Monoclonal Antibody (MA5-16949, 1:100, Invitrogen, USA) (overnight, RT). Following three washes with PBS and culture in Goat Anti-Mouse IgG H&L (ab205719, 1:7000, Abcam, UK) (RT, 15 min), the sections were colored with Aminoethyl Carbazole (AEC, 001122, ThermoFisher Scientific, USA) and counterstained with Mayer's Hematoxylin (AR-0712, Beijing DingGuoChang-Sheng Biotech, China). Using the microscope, the images of the wound area (magnification $\times$100, scale bar = 50 µm) were immediately analyzed using the Image-Pro Plus 6.0 software.

Sirius Red Staining Assay

To quantify collagen production *in vitro*, a Picro-Sirius Red staining assay was performed. HSFs were seeded in 24-well plates and treated with TGF-β1 or breviscapine (48 h) based on grouping. After two washes with PBS, cells underwent fixation (4% paraformaldehyde; 30 min, RT), washing (PBS; twice), and staining (Picro-Sirius Red Solution; ab246832, Abcam, UK; 37 °C, 90 min). The plates were rinsed in tap water and then dried in air. Then, Sirius Red staining solution was dissolved in 0.1 M Sodium hydroxide solution (58300C, Sigma-Aldrich, USA). Finally, the absorbance was measured at 540 nm using a SpectraMax 190 microplate reader.

Statistical Analysis

Statistical analyses were performed using GraphPad 8.0 software (GraphPad Software, Inc., San Diego, CA, USA). All data are expressed as mean $\pm$ standard deviation (SD). The normality of data was assessed using the Shapiro-Wilk test. No significant deviation from normality was detected. Multi-group comparisons were implemented using one-way analysis of variance (one-way ANOVA), followed by Tukey post-hoc test. p-values < 0.05 were deemed statistically significant.

Results

Breviscapine Attenuated Scar Formation and Reduced the mRNA and Protein Expression of Fibrosis-Related Markers in Vivo

In this study, the effects of breviscapine on HS *in vivo* were investigated by establishing a rabbit ear HS model. Fig. 1a shows the chemical structure of breviscapine. After 28 days of treatment with breviscapine, we preliminarily observed the appearance of scar tissues. In the control group, rabbit exhibited normal, scar-free ears; in the HS group, the scar was stiff, red and prominent; in the BE-L group, the scar was reduced and still raised with light red; in the BE-M group, the scar was significantly reduced, softer, and less obvious; in the BE-H group, the scar was almost invisible, with color nearly matching the surrounding normal tissue (Fig. 1b). The mRNA expression levels of fibrosis-related markers (COL1A1, COL3A1 and ACTA1) were quantified by qRT-PCR and found to be upregulated after modeling ($p < 0.001$, Fig. 1c–e). In contrast, after breviscapine treatment, the relative mRNA expression levels of the fibrosis-related markers were decreased ($p < 0.001$, Fig. 1c–e). The relative protein expression levels of fibrosis-related markers, including collagen I, collagen III, and α-SMA, were measured using Western blotting, which were markedly elevated in the HS group ($p < 0.001$, Fig. 1f,g). However, their expression levels were lower in the BE-L, BE-M and BE-H groups than in the HS group ($p < 0.001$, Fig. 1f,g).

Breviscapine Reduced α-SMA and TGF-β1 Expression, and Ameliorated the Excessive Density and Irregular Arrangement of Collagen Fibers in Vivo

α-SMA expression *in vivo* was observed using immunofluorescence staining. The data revealed α-SMA level was enhanced after HS induction, which was reversed by breviscapine dose-dependently ($p < 0.001$, Fig. 2a,b). Masson trichrome staining data indicated the collagen fibers were normal in the control group, but exhibited high density and irregular arrangement in the HS group. All breviscapine treatment groups showed reduced fiber density and more orderly arrangement (Fig. 2c). The collagen area was significantly elevated in the HS group relative to the control group ($p < 0.001$, Fig. 2d); in contrast, it was markedly reduced in the BE-L, BE-M and BE-H groups compared to the HS group ($p < 0.001$, Fig. 2d). Immunohistochemistry data confirmed that TGF-β1 expression was significantly increased due to modeling, but was dose-dependently diminished by breviscapine ($p < 0.001$, Fig. 2e,f). Through western blotting, we detected that TGF-β1 expression was decreased in the BE-related groups, relative to the HS group ($p < 0.001$, Fig. 2g,h).

Breviscapine Inhibited Cell Viability and Reversed the Stimulating Effect of TGF-β on Collagen Production in HSFs

Different concentrations of breviscapine (2.5, 5, 10, 15 µM) were used to treat HSFs, and cell viability detection was conducted with a CCK-8 assay at 24 and 48 h. Since breviscapine decreased cell viability dose-dependently ($p < 0.05$, Fig. 3a), 15 µM of breviscapine was used to treat HSFs for 48 h in the subsequent experiments. The relative collagen production was detected using Sirius Red staining, revealing that the production was significantly enhanced by TGF-β1 intervention ($p < 0.001$, Fig. 3b,c), whereas breviscapine markedly attenuated this effect ($p < 0.001$, Fig. 3b,c). Western blotting indicated that fibrosis-related marker protein expression levels were increased in the TGF-β1 group ($p < 0.01$, Fig. 3d,e); in contrast, the expression levels were reduced in the TGF-β1+BE group ($p < 0.05$, Fig. 3d,e).

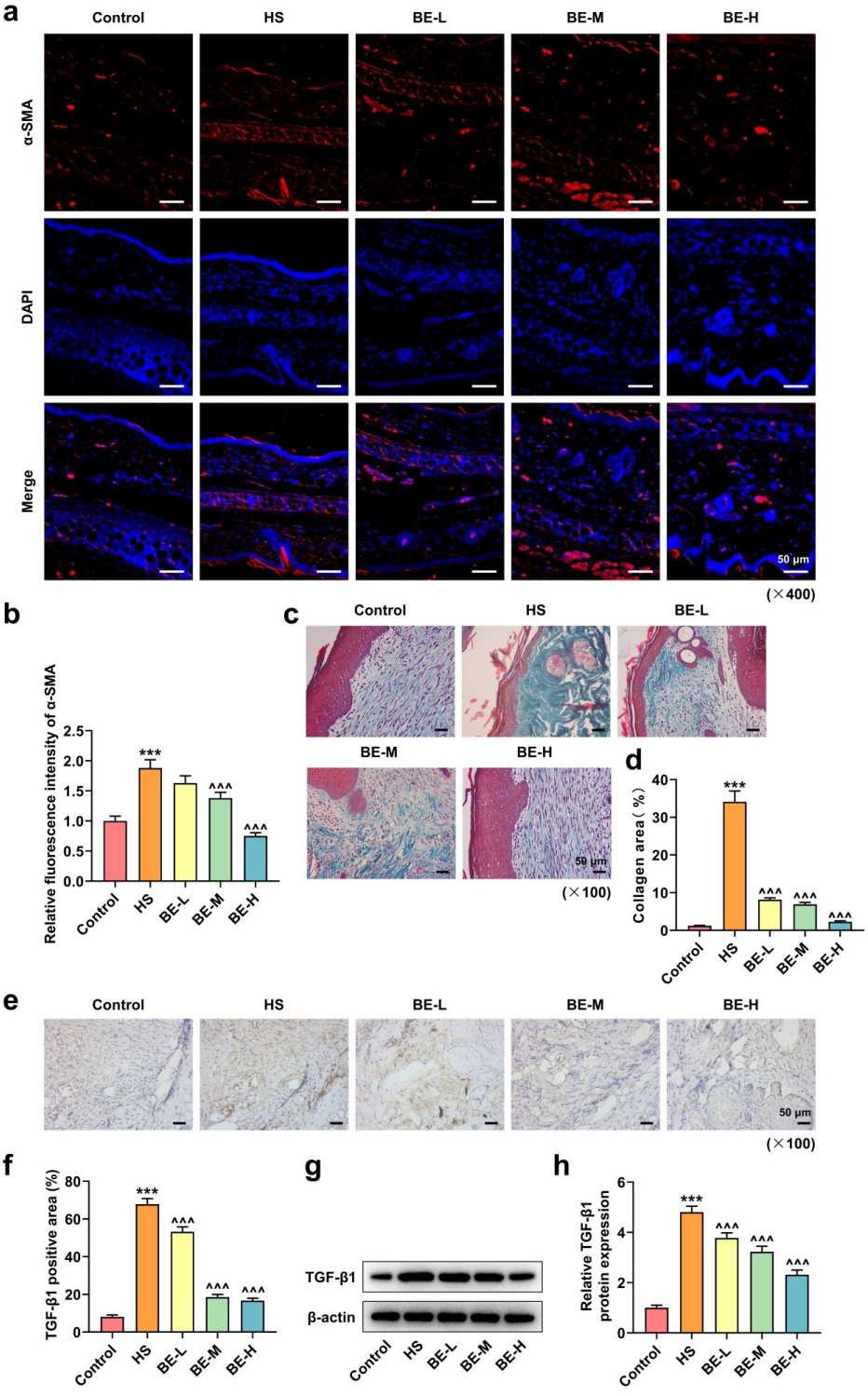

Fig. 2. The effects of breviscapine on α-SMA and TGF-β1 expression, and the density and arrangement of collagen fibers *in vivo*. (a,b) After 28-day breviscapine treatment, the images of alpha-smooth muscle actin (α-SMA) (red) in scar tissues on the rabbit ear HS model, including the control (n = 6), HS (n = 6), BE-L (n = 6), BE-M group (n = 6), and BE-H groups (n = 6) (immunofluorescence staining assay; magnification ×400, scale bar = 50 μm). (c,d) Collagen fibers after 28-day breviscapine treatment (Masson staining assay; magnification ×100, scale bar = 50 μm). (e,f) Transforming growth factor-β1 (TGF-β1) expression (immunohistochemistry; magnification ×100, scale bar = 50 μM) after breviscapine treatment. (g,h) TGF-β1 protein expression (Western blotting, β-actin as the housekeeping gene). All experiments were performed in triplicate, with data presented as mean ± SD (n = 6 rabbits/group). $^{***}p < 0.001$ vs. Control; $^{\wedge\wedge\wedge}p < 0.001$ vs. HS. Abbreviation: HS, hypertrophic scar; BE-L, breviscapine-low dose; BE-M, breviscapine-medium dose; BE-H, breviscapine-high dose.

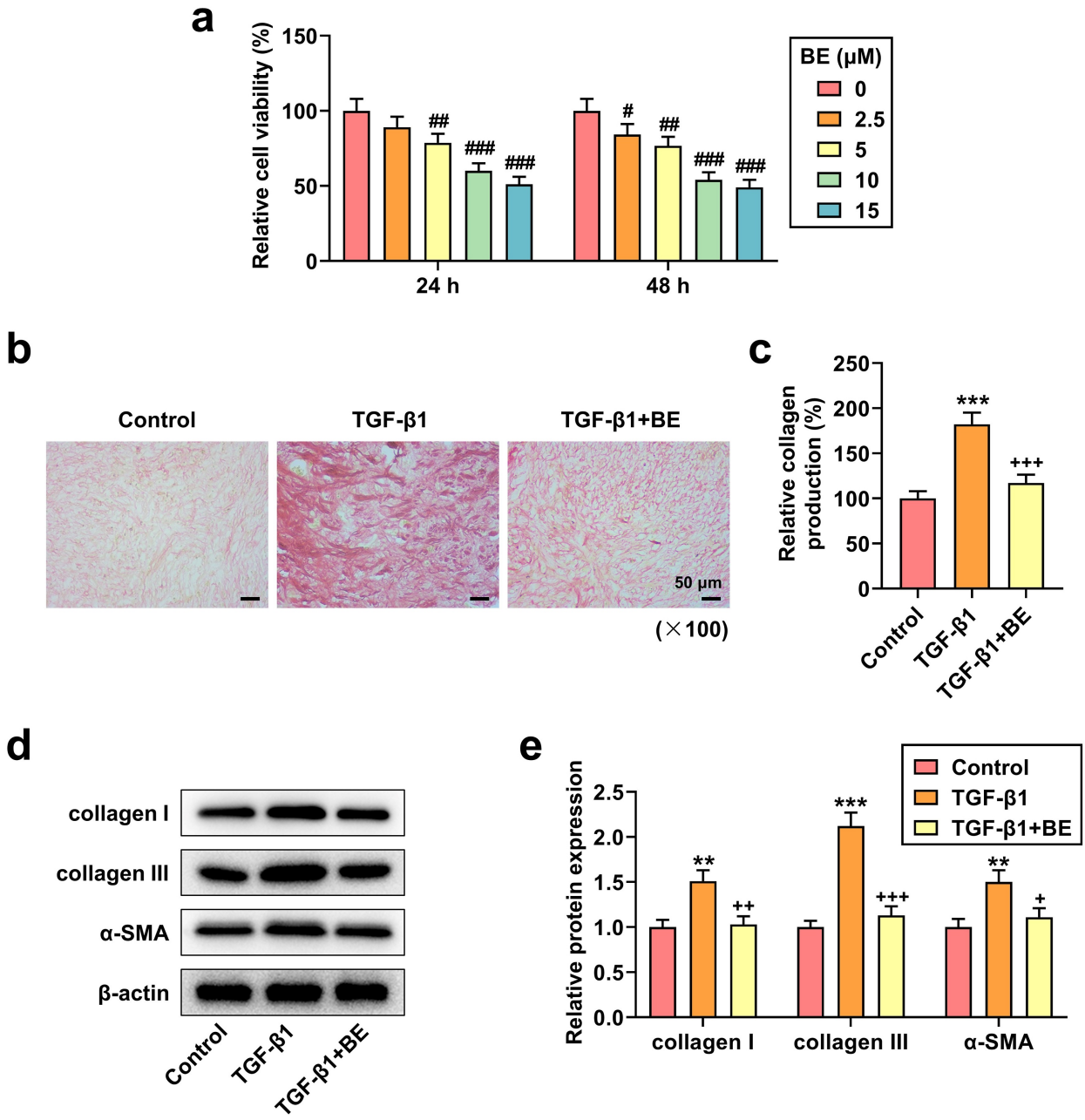

Fig. 3. The effects of breviscapine on cell viability and collagen production induced by TGF-β1 in HSFs. (a) Cell viability in HSFs (CCK-8). (b,c) The relative collagen production (Sirius Red staining; magnification ×100, scale bar = 50 μm). (d,e) The protein expression levels of fibrosis-related markers (collagen I, collagen III and α-SMA) (Western blotting, β-actin as the housekeeping gene). Data are presented as mean ± SD. Each experiment was repeated thrice independently (n = 3). $^{\#}p < 0.05$; $^{\#\#}p < 0.01$; $^{\#\#\#}p < 0.001$ vs. 0; $^{**}p < 0.01$; $^{***}p < 0.001$ vs. Control;$^{+}p < 0.05$; $^{++}p < 0.01$; $^{+++}p < 0.001$ vs. TGF-β1. Abbreviation: HSFs, hypertrophic scar fibroblasts; CCK-8, cell counting kit-8.

Breviscapine Dampened the Protein Expression of TGF-β1 and the Akt-mTOR Pathway in HSFs

We confirmed through Western blotting that the protein expression levels of TGF-β1, p-Akt and p-mTOR were increased ($p < 0.001$), and those of Akt and mTOR remained unchanged following TGF-β1 intervention (Fig. 4a,b). Due to the co-treatment of breviscapine, the protein expression levels of TGF-β1, p-Akt and p-mTOR were decreased ($p < 0.01$), and those of Akt and mTOR remained unchanged (Fig. 4a,b). Moreover, TGF-β1 intervention resulted in elevated ratios of p-mTOR/mTOR and p-Akt/Ak ($p < 0.01$), while the ratios were decreased by co-treatment of breviscapine ($p < 0.01$, Fig. 4c,d).

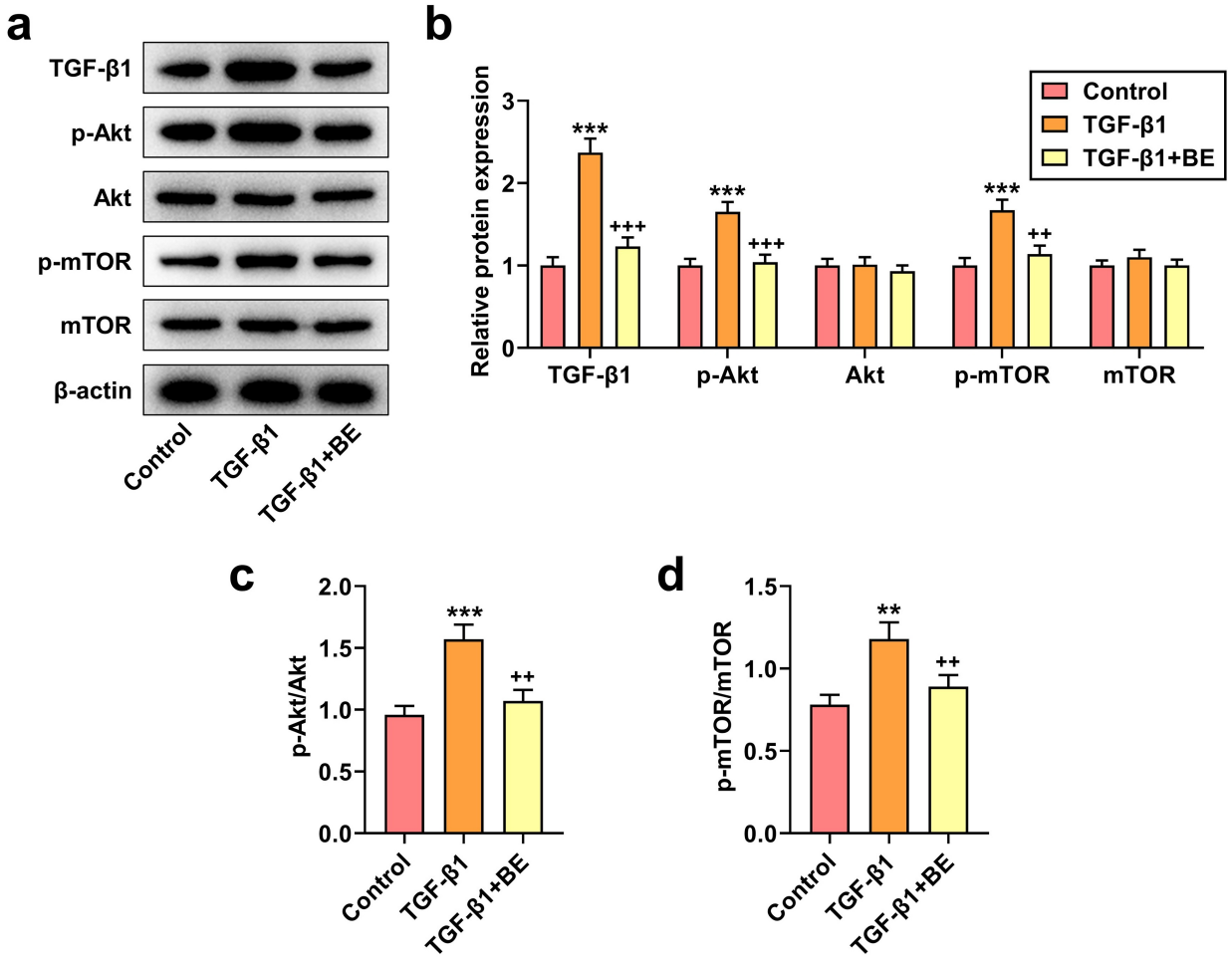

Fig. 4. The effects of breviscapine on the protein expression of TGF-β1 and Akt-mTOR pathway. (a,b) Protein expression levels of TGF-β1, p-Akt, p-mTOR, Akt and mTOR (Western blotting, β-actin as the housekeeping gene). (c,d) Ratios of p-mTOR/mTOR and p-Akt/Ak (β-actin as the housekeeping gene). Each experiment was repeated thrice independently (n = 3), with data expressed as mean $\pm$ SD. $^{**}p < 0.01$; $^{***}p < 0.001$ vs. Control; $^{++}p < 0.01$; $^{+++}p < 0.001$ vs. TGF-β1. Abbreviation: p-Akt, phosphorylated-Akt; mTOR, mammalian target of rapamycin; p-mTOR, phosphorylated mTOR.

Discussion

HS represents a persistent clinical challenge and affects the health of millions of people both physically and psychologically, thus drawing global attention [30,31]. Despite advances in current medical management and research results, countless HS patients continue to experience substantial pain and suffering every year. Interestingly, accumulating evidence indicates that breviscapine generates anti-inflammatory and anti-fibrotic effects in several diseases, including cardiovascular diseases [32]. Owing to these established properties, breviscapine has been widely recognized as a valuable ingredient in clinical treatment [33,34]. To clarify the influence of breviscapine on HS, we constructed a rabbit ear HS model and found that breviscapine dose-dependently reduced scars, making them softer and less obvious.

TGF-β1, implicated in both physiological repair and collagen accumulation, was originally identified in the study of cancer cell processes [35]. Our study confirmed that breviscapine effectively downregulated TGF-β1 in HS tissues and HSFs, while inhibiting cell viability and reversing the stimulating effect of TGF-β1 on collagen production in HSFs. These findings aligned with the reported action of other natural compounds in HS, such as curcumin, artesunate and ellagic acid, which also exert anti-fibrotic effects through TGF-β1 suppression. For instance, curcumin inhibits fibroblast activation and tissue inflammation to mitigate HS [36]; in a rabbit ear HS model, artesunate has been shown to achieved the promotion of wound healing, alleviation of path morphologial change in scar tissue, and reduction of ECM production by suppressing the TGF-β1/Smad3 signaling pathway [37]; likewise, ellagic acid suppresses the formation of HS by suppressing TGF-β/Smad signaling pathway activity [38]. In addition, ACTA1 belongs to the human actin family, which is associated with muscle contraction and is one of the markers of fibrosis [39]. Collagen proteins, COL1A1 and COL3A1, also serve as es-

sential biomarkers in wound healing assays [40]. α-SMA, a hallmark of myofibroblasts, has the ability to promote scar recovery [41]. Therefore, in our experiment, we focused on these fibrosis-related markers such as ACTA1, α-SMA, COL1A1 and COL3A1. *In vivo*, breviscapine significantly downregulated key fibrotic markers at both mRNA (COL1A1, COL3A1, ACTA1) and protein (collagen I, collagen III, α-SMA) levels, and improved collagen fiber architecture. The *in vitro* data further supported these findings, showing that breviscapine inhibited HSF proliferation and TGF-β1-induced collagen overproduction.

This study first evidenced that breviscapine concurrently suppressed the Akt-mTOR pathway and TGF-β1 axis in HS. Reportedly, the Akt-mTOR pathway is implicated in the regulation of the actin cytoskeleton and autophagy [42]. The activation of the Akt pathway could also accelerate the formation of HS [43]. Gluconic acid binds to PLOD1, attenuates p-AKT signaling, and enhances autophagy to alleviate HS formation [44]. Additionally, breviscapine reduces fibrosis by suppressing inflammation and mediating TGF and Smad signaling pathways, and the role of TGF in abdominal adhesion cannot be underestimated [28]. Breviscapine has also been reported to block the Akt pathway [45]. TGF-β1-induced up-regulation of the Akt pathway is repressed by pentoxifylline in HS [46]. The crosstalk between TGF-β1 and Akt-mTOR signaling forms a potent pro-fibrotic axis. Breviscapine was observed to suppress both TGF-β1 and p-Akt/p-mTOR in our *in vitro* experiments, representing a distinct and potentially more comprehensive mechanism compared to agents targeting a single pathway.

The precise upstream molecular target of breviscapine responsible for this dual inhibition warrants further investigation. We proposed several plausible mechanisms based on existing literature: (1) Breviscapine may directly or indirectly modulate upstream membrane receptors of both pathways, such as TGF-β receptors or integrins, thereby attenuating initial signal activation. (2) It may activate upstream negative regulators like PTEN (a phosphatase that inhibits PI3K/Akt) or AMPK (an energy sensor that inhibits mTORC1), leading to downstream suppression. (3) Its antioxidant properties could mitigate reactive oxygen species (ROS), which are known activators of both TGF-β1 and PI3K/Akt signaling in fibrotic contexts. However, these proposed mechanisms still require further analysis in future studies.

Several limitations in this study should be acknowledged. Firstly, the rabbit ear HS model, while well-established, does not fully recapitulate the complex pathophysiology and chronic progression of human HS, particularly the role of immune cells and tension over larger body surfaces. Secondly, the therapeutic regimen was limited to localized subcutaneous injection, which may not reflect systemic or topical delivery routes. The efficacy and safety of these alternative formulations require additional investigation. Thirdly, the long-term safety profile of breviscapine, potential systemic effects, and the durability of its anti-scarring effects beyond the observation period remain unknown. In addition, we did not perform experiments using specific agonists of TGF-β1 and Akt-mTOR pathways to determine whether reactivating the pathways could reverse the anti-fibrotic effects of breviscapine. Finally, the precise mechanism by which breviscapine interacts with the TGF-β1 and Akt-mTOR pathways remains unexplored, and further studies are needed to clarify its primary molecular target(s).

To advance its clinical translation, future research should focus on: (1) developing and optimizing patient-friendly topical or sustained-release delivery systems; (2) conducting comprehensive evaluations regarding long-term efficacy and systemic safety in relevant animal models; (3) employing rescue experiments with pathway agonists to conclusively validate the causal role of TGF-β1/Akt-mTOR inhibition in breviscapine's mechanisms; (4) and elucidating the precise upstream molecular target(s) of breviscapine to enable potential structure-based optimization.

Conclusion

Collectively, our findings demonstrate that breviscapine attenuates HS formation by inhibiting the key pro-fibrotic TGF-β1 signaling and the Akt-mTOR pathway, thereby reducing myofibroblast activation and collagen overproduction, and improving scar morphology. This dual-target strategy offers a new perspective for the development of multi-target anti-scarring agents and highlights breviscapine as a uniquely promising candidate worthy of further translational investigation.

Availability of Data and Materials

The analyzed data sets generated during the study are available from the corresponding author on reasonable request.

Author Contributions

PG and QG designed the research study. LL performed the research. LL and PG collected and analyzed the data. QG has been involved in drafting the manuscript and all authors have been involved in revising it critically for important intellectual content. All authors gave final approval of the version to be published. All authors have participated sufficiently in the work to take public responsibility for appropriate portions of the content and agreed to be accountable for all aspects of the work in ensuring that questions related to its accuracy or integrity.

Ethics Approval and Consent to Participate

The study was approved by the Laboratory Animal Ethics Review Committee of Shandong Provincial Hospital Affiliated to Shandong First Medical University (No. HSRF (preliminary application) 2024-0027).

Acknowledgment

Not applicable.

Funding

This study was supported by the Investigation on the Expression Profiles and Underlying Mechanisms of Key Genes in Hypertrophic Scar Pathogenesis Based on Single-Cell Sequencing horizontal project of Shandong Provincial Hospital.

Conflict of Interest

The authors declare no conflict of interest.

References

[1] Bharadia SK, Burnett L, Gabriel V. Hypertrophic Scar. Physical Medicine and Rehabilitation Clinics of North America. 2023; 34: 783–798. https://doi.org/10.1016/j.pmr.2023.05.002.

[2] Yin J, Zhang S, Yang C, Wang Y, Shi B, Zheng Q, *et al*. Mechanotransduction in skin wound healing and scar formation: Potential therapeutic targets for controlling hypertrophic scarring. Frontiers in Immunology. 2022; 13: 1028410. https://doi.org/10.3389/fimmu.2022.1028410.

[3] Li J, Yin Y, Zhang E, Gui M, Chen L, Li J. Peptide deregulated in hypertrophic scar-1 alleviates hypertrophic scar fibrosis by targeting focal adhesion kinase and pyruvate kinase M2 and remodeling the metabolic landscape. International Journal of Biological Macromolecules. 2023; 235: 123809. https://doi.org/10.1016/j.ijbiomac.2023.123809.

[4] Mony MP, Harmon KA, Hess R, Dorafshar AH, Shafikhani SH. An Updated Review of Hypertrophic Scarring. Cells. 2023; 12: 678. https://doi.org/10.3390/cells12050678.

[5] Shang RY, Yang JC, Hu WG, Xiao R, Hu DS, Lin ZC, *et al*. Artesunate attenuates skin hypertrophic scar formation by inhibiting fibroblast activation and EndMT of vascular endothelial cells. Phytomedicine. 2025; 140: 156498. https://doi.org/10.1016/j.phymed.2025.156498.

[6] Jiang Q, Chen J, Tian F, Liu Z. Silicone gel sheeting for treating hypertrophic scars. The Cochrane Database of Systematic Reviews. 2021; 9: CD013357. https://doi.org/10.1002/14651858.CD013357.pub2.

[7] Santuzzi CH, Gonçalves Liberato FM, Fachini de Oliveira NF, Sgrancio do Nascimento A, Nascimento LR. Massage, laser and shockwave therapy improve pain and scar pruritus after burns: a systematic review. Journal of Physiotherapy. 2024; 70: 8–15. https://doi.org/10.1016/j.jphys.2023.10.010.

[8] Qiu H, Wu B, Pan F, Zhou S, Zhang L, Zhou X. Manual Fractional Technology with CO_2 Laser Combined with Transdermal Drug Delivery for Hypertrophic Scar: A Retrospective Study. Aesthetic Plastic Surgery. 2025; 49: 3756–3766. https://doi.org/10.1007/s00266-025-04837-5.

[9] Zhou T, Chen Y, Wang C, Huang Z, Tan Z, Ma Y. SIRT6 Inhibits the Proliferation and Collagen Synthesis of Keloid Fibroblasts through MAPK/ERK Pathway. Discovery Medicine. 2024; 36: 1430–1440. https://doi.org/10.24976/Discov.Med.202436186.133.

[10] Gao Y, Liu Y, Zheng D, Ho C, Wen D, Sun J, *et al*. HDAC5-mediated Smad7 silencing through MEF2A is critical for fibroblast activation and hypertrophic scar formation. International Journal of Biological Sciences. 2022; 18: 5724–5739. https://doi.org/10.7150/ijbs.76140.

[11] Hilliard BA, Amin M, Popoff SN, Barbe MF. Potentiation of Collagen Deposition by the Combination of Substance P with Transforming Growth Factor Beta in Rat Skin Fibroblasts. International Journal of Molecular Sciences. 2024; 25: 1862. https://doi.org/10.3390/ijms25031862.

[12] Wang Y, Zhang Y, Li J, Li C, Zhao R, Shen C, *et al*. Hypoxia Induces M2 Macrophages to Express VSIG4 and Mediate Cardiac Fibrosis After Myocardial Infarction. Theranostics. 2023; 13: 2192–2209. https://doi.org/10.7150/thno.78736.

[13] Li YH, Yang J, Zheng Z, Hu DH, Wang ZD. Botulinum toxin type A attenuates hypertrophic scar formation via the inhibition of TGF-β1/Smad and ERK pathways. Journal of Cosmetic Dermatology. 2021; 20: 1374–1380. https://doi.org/10.1111/jocd.13842.

[14] Tang F, Gong H, Ke T, Yang W, Yang Y, Liu Z. USP7 Promotes TGF-β1 Signaling by De-Ubiquitinating Smad2/Smad3 in Pulmonary Fibrosis. Discovery Medicine. 2024; 36: 1616–1626. https://doi.org/10.24976/Discov.Med.202436187.148.

[15] Shi W, Wu Y, Bian D. p75NTR silencing inhibits proliferation, migration, and extracellular matrix deposition of hypertrophic scar fibroblasts by activating autophagy through inhibiting the PI3K/Akt/mTOR pathway. Canadian Journal of Physiology and Pharmacology. 2021; 99: 349–359. https://doi.org/10.1139/cjpp-2020-0219.

[16] Chen H, Xu K, Sun C, Gui S, Wu J, Wang S. Inhibition of ANGPT2 activates autophagy during hypertrophic scar formation via PI3K/AKT/mTOR pathway. Anais Brasileiros De Dermatologia. 2023; 98: 26–35. https://doi.org/10.1016/j.abd.2021.12.005.

[17] Zhao S, Liu H, Wang H, He X, Tang J, Qi S, *et al*. Inhibition of phosphatidylinositol 3-kinase catalytic subunit alpha by miR-203a-3p reduces hypertrophic scar formation via phosphatidylinositol 3-kinase/AKT/mTOR signaling pathway. Burns & Trauma. 2024; 12: tkad048. https://doi.org/10.1093/burnst/tkad048.

[18] Dong Y, Cao X, Huang J, Hu Z, Chen C, Chen M, *et al*. Melatonin inhibits fibroblast cell functions and hypertrophic scar formation by enhancing autophagy through the MT2 receptor-inhibited PI3K/Akt /mTOR signaling. Biochimica et Biophysica Acta. Molecular Basis of Disease. 2024; 1870: 166887. https://doi.org/10.1016/j.bbadis.2023.166887.

[19] Tang Q, Markby GR, MacNair AJ, Tang K, Tkacz M, Parys M, *et al*. TGF-β-induced PI3K/AKT/mTOR pathway controls myofibroblast differentiation and secretory phenotype of valvular interstitial cells through the modulation of cellular senescence in a naturally occurring in vitro canine model of myxomatous mitral valve disease. Cell Proliferation. 2023; 56: e13435. https://doi.org/10.1111/cpr.13435.

[20] Younes B, Mandour E, Soliman Hashish M, Gamal Shoukr T. The efficacy of fractional CO_2 laser with or without triamcinolone acetonide or 5-fluorouracil in the treatment of early post-burn hypertrophic scars. Lasers in Medical Science. 2025; 40: 33. https://doi.org/10.1007/s10103-024-04256-z.

[21] Kim S, Woo YR, Cho SH, Lee JD, Kim HS. Clinical Efficacy of 5-Fluorouracil and Bleomycin in Dermatology. Journal of Clinical Medicine. 2024; 13: 335. https://doi.org/10.3390/jcm13020335.

[22] Wen L, He T, Yu A, Sun S, Li X, Wei J, *et al*. Breviscapine: A

Review on its Phytochemistry, Pharmacokinetics and Therapeutic Effects. The American Journal of Chinese Medicine. 2021; 49: 1369–1397. https://doi.org/10.1142/S0192415X21500646.

[23] Niu P, Liu F, Lei F, Peng J, Wang Y, Zhao J, *et al*. Breviscapine regulates the proliferation, migration, invasion, and apoptosis of colorectal cancer cells via the PI3K/AKT pathway. Scientific Reports. 2023; 13: 9674. https://doi.org/10.1038/s41598-023-33792-x.

[24] Song J, Zhang J, Shi J, Pan X, Mo D. Breviscapine Reduces Sepsis-Induced Acute Lung Injury by Targeting CASP8 to Regulate Neutrophil Apoptosis and Inflammation. Journal of Inflammation Research. 2024; 17: 5161–5176.

[25] Lan T, Jiang S, Zhang J, Weng Q, Yu Y, Li H, *et al*. Breviscapine alleviates NASH by inhibiting TGF-β-activated kinase 1-dependent signaling. Hepatology. 2022; 76: 155–171. https://doi.org/10.1002/hep.32221.

[26] Li WQ, Liu WH, Qian D, Liu J, Zhou SQ, Zhang L, *et al*. Traditional Chinese medicine: An important source for discovering candidate agents against hepatic fibrosis. Frontiers in Pharmacology. 2022; 13: 962525. https://doi.org/10.3389/fphar.2022.962525.

[27] Yang X, Xiao Y, Zhong C, Shu F, Xiao S, Zheng Y, *et al*. ABT-263 Reduces Hypertrophic Scars by Targeting Apoptosis of Myofibroblasts. Frontiers in Pharmacology. 2021; 11: 615505. https://doi.org/10.3389/fphar.2020.615505.

[28] Zhang H, Song Y, Li Z, Zhang T, Zeng L. Evaluation of breviscapine on prevention of experimentally induced abdominal adhesions in rats. American Journal of Surgery. 2016; 211: 1143–1152. https://doi.org/10.1016/j.amjsurg.2015.05.037.

[29] Livak KJ, Schmittgen TD. Analysis of relative gene expression data using real-time quantitative PCR and the 2(-Delta Delta C(T)) Method. Methods. 2001; 25: 402–408. https://doi.org/10.1006/meth.2001.1262.

[30] Li Y, Zhang J, Shi J, Liu K, Wang X, Jia Y, *et al*. Exosomes derived from human adipose mesenchymal stem cells attenuate hypertrophic scar fibrosis by miR-192-5p/IL-17RA/Smad axis. Stem Cell Research & Therapy. 2021; 12: 221. https://doi.org/10.1186/s13287-021-02290-0.

[31] Nabai L, Pourghadiri A, Ghahary A. Hypertrophic Scarring: Current Knowledge of Predisposing Factors, Cellular and Molecular Mechanisms. Journal of Burn Care & Research. 2020; 41: 48–56. https://doi.org/10.1093/jbcr/irz158.

[32] Chen ZQ, Zhou Y, Chen F, Huang JW, Zheng J, Li HL, *et al*. Breviscapine Pretreatment Inhibits Myocardial Inflammation and Apoptosis in Rats After Coronary Microembolization by Activating the PI3K/Akt/GSK-3β Signaling Pathway. Drug Design, Development and Therapy. 2021; 15: 843–855. https://doi.org/10.2147/DDDT.S293382.

[33] Wu R, Liang Y, Xu M, Fu K, Zhang Y, Wu L, *et al*. Advances in Chemical Constituents, Clinical Applications, Pharmacology, Pharmacokinetics and Toxicology of *Erigeron breviscapus*. Frontiers in Pharmacology. 2021; 12: 656335. https://doi.org/10.3389/fphar.2021.656335.

[34] Wen L, He T, Yu A, Sun S, Li X, Wei J, *et al*. Breviscapine: A Review on its Phytochemistry, Pharmacokinetics and Therapeutic Effects. American Journal of Chinese Medicine. 2021; 49: 1369–1397. https://doi.org/10.1142/S0192415X21500646.

[35] de Streel G, Lucas S. Targeting immunosuppression by TGF-β1 for cancer immunotherapy. Biochemical Pharmacology. 2021; 192: 114697. https://doi.org/10.1016/j.bcp.2021.114697.

[36] Fei H, Qian Y, Pan T, Wei Y, Hu Y. Curcumin alleviates hypertrophic scarring by inhibiting fibroblast activation and regulating tissue inflammation. Journal of Cosmetic Dermatology. 2023; 23: 227–235. https://doi.org/10.1111/jocd.15905.

[37] Nong X, Rajbanshi G, Chen L, Li J, Li Z, Liu T, *et al*. Effect of artesunate and relation with TGF-β1 and SMAD3 signaling on experimental hypertrophic scar model in rabbit ear. Archives of Dermatological Research. 2019; 311: 761–772. https://doi.org/10.1007/s00403-019-01960-7.

[38] Zhao ZJ, Wu DJ, Lv DL, Zhang BD, Chen L, Sun YQ. Ellagic acid inhibits the formation of hypertrophic scars by suppressing TGF-β/Smad signaling pathway activity. Chemical Biology & Drug Design. 2023; 102: 773–781. https://doi.org/10.1111/cbdd.14287

[39] Matsumoto A, Tsuda H, Furui S, Kawada-Nagashima M, Anzai T, Seki M, *et al*. A case of congenital fiber-type disproportion syndrome presenting dilated cardiomyopathy with ACTA1 mutation. Molecular Genetics & Genomic Medicine. 2022; 10: e2008. https://doi.org/10.1002/mgg3.2008.

[40] Lee JE, Boo YC. Combination of Glycinamide and Ascorbic Acid Synergistically Promotes Collagen Production and Wound Healing in Human Dermal Fibroblasts. Biomedicines. 2022; 10: 1029. https://doi.org/10.3390/biomedicines10051029.

[41] Lyu SC, Wang J, Xu WL, Wang HX, Pan F, Jiang T, *et al*. Therapeutic Effect of Combining Anisodamine With Neostigmine on Local Scar Formation Following Roux-en-Y Choledochojejunostomy in a Novel Rat Model. Frontiers in Pharmacology. 2021; 12: 700050. https://doi.org/10.3389/fphar.2021.700050.

[42] Liu C, Hu X, Zhao Y, Huang A, Chen J, Lu T, *et al*. High-Glucose-Induced Injury to Proximal Tubules of the Renal System Is Alleviated by Netrin-1 Suppression of Akt/mTOR. Journal of Diabetes Research. 2023; 2023: 4193309. https://doi.org/10.1155/2023/4193309.

[43] Ma F, Shen J, Zhang H, Zhang Z, Yang A, Xiong J, *et al*. A novel lncRNA FPASL regulates fibroblast proliferation via the PI3K/AKT and MAPK signaling pathways in hypertrophic scar. Acta Biochimica et Biophysica Sinica. 2022; 55: 274–284. https://doi.org/10.3724/abbs.2022122.

[44] Li J, Zeng S, Sun Y, Zou J, Zhang E, Yan Q, *et al*. Gluconic acid alleviates hypertrophic scar formation through binding PLOD1, reducing p-AKT signaling and activating autophagy. Phytomedicine. 2025; 143: 156825. https://doi.org/10.1016/j.phymed.2025.156825.

[45] Jiang W, Li Z, Zhao W, Chen H, Wu Y, Wang Y, *et al*. Breviscapine attenuatted contrast medium-induced nephropathy via PKC/Akt/MAPK signalling in diabetic mice. American Journal of Translational Research. 2016; 8: 329–341.

[46] Yang F, Chen E, Yang Y, Han F, Han S, Wu G, *et al*. The Akt/FoxO/p27^{Kip1} axis contributes to the anti-proliferation of pentoxifylline in hypertrophic scars. Journal of Cellular and Molecular Medicine. 2019; 23: 6164–6172. https://doi.org/10.1111/jcmm.14498.